Checkerboard pattern of the interlayer coupling between two Co films across Fe/Cu and Cu/Co/Cu spacer layers grown on Cu(100)

Y. Z. Wu,[1] C. Y. Won,[1] E. Rotenberg,[2] H. W. Zhao,[1,3] N. V. Smith,[2] and Z. Q. Qiu[1,4]
[1]*Department of Physics, University of California, Berkeley, California 94720, USA*
[2]*Advanced Light Source, Lawrence Berkeley National Laboratory, Berkeley, California 94720, USA*
[3]*International Center for Quantum Structures, Institute of Physics, Chinese Academy of Sciences, Beijing 100080, China*
[4]*Materials Science Division, Lawrence Berkeley National Laboratory, Berkeley, California 94720, USA*
(Received 4 November 2003; revised manuscript received 1 March 2004; published 8 June 2004)

Quantum well (QW) states and oscillatory interlayer coupling in Co/Cu/Fe/Co/Cu(001) are investigated by angular resolved photoemission spectroscopy and x-ray magnetic linear dichroism. We find that the QW states in Cu/Fe/Co/Cu(001) depend very little on the magnetic state of the fcc Fe films. The interlayer coupling between the Co films across the Cu/Fe spacer layer displays a checkerboard pattern in Fe-Cu thickness plane. The presence of the fcc Fe ferromagnetic live layer at the Cu/Fe interface is shown to be responsible for the checkerboard pattern, which was confirmed by experiments on Co/Cu/Co/Cu/Co/Cu(100) system.

DOI: 10.1103/PhysRevB.69.214410 PACS number(s): 75.75.+a

I. INTRODUCTION

Oscillatory magnetic interlayer coupling[1,2] is a phenomenon in which magnetic coupling between two ferromagnetic layers across a nonferromagnetic spacer oscillates with the spacer layer thickness. Understanding the coupling mechanism has attracted a great interest for research because of its fundamental importance. After magnetic measurements[3–5] showed that the interlayer coupling strength depends on the ferromagnetic layer thickness, research on the physical origin of the interlayer coupling went beyond the Rudermann-Kittel-Kasuya-Yosida (RKKY) interactions. In particular, the discovery of the quantum well (QW) states in a thin Cu film on ferromagnetic Co with long[6] and short periodicities[7,8] led to the reexamination of the coupling mechanism in terms of electron confinement in the spacer layer.[9–11] Great progress has been made by photoemission experiments which not only identified quantum interference as a function of the ferromagnetic layer thickness,[12] but also explained quantitatively the long- and short-period interlayer coupling oscillations in terms of momentum resolved QW states.[13] Recently, research on the interlayer coupling has been developed along two directions. In terms of materials, research has been extended from metallic spacer layer to semiconductor[14,15] and insulator.[16,17] In terms of spacer layer structure, doping[18] and multilayers have been used to modify the interlayer coupling.[19,20] Multilayer spacer can be regarded as a multi QW system, and indeed interlayer coupling between two Co films across double QW $Cu/Ni_{30}Cu_{70}/Cu$ spacer layer was found to follow exactly the QW states at the Fermi level (E_F).[21] In the previous studies, the spacer layer is usually made of nonferromagnetic elements so that its intrinsic electronic structure is spin independent. Since QW coupling comes from spin-dependent electron confinement, it will be very interesting to ask: how the interlayer coupling behaves if the spacer layer consists of ferromagnetic element? To answer this question, we investigated the QW states in Cu/Fe/Co/Cu(100) system and the interlayer coupling in Co/Cu/Fe/Co/Cu(100) system in which the Cu/Fe serves as the spacer layer.

Face-centered-cubic (fcc) Fe film grown on Cu(100) attracted great attention because it exhibits many interesting structural and magnetic phases.[22,23] The room temperature grown fcc Fe film is ferromagnetic below 4 ML (monolayer), and antiferromagnetic plus a ferromagnetic surface live layer with fct structure between 4 and 11 ML.[24,25] It was also shown that fcc Fe grown on Co/Cu(100) exhibits very similar structural and magnetic behavior as in the Fe/Cu(100) system.[26–31] However, the location of the magnetic live layer at the surface of fcc Fe film remains somewhat controversial in Fe/Co/Cu(100). Oxygen absorption experiments[26,27] suggest that the ferromagnetic live layer is located at the Fe/Co interface. In particular, x-ray magnetic dichroism measurement shows that there is no ferromagnetic Fe surface layer at room temperature.[26] However, photoemission dichroism experiment at low temperature shows that the ferromagnetic live layer is at the Fe surface.[28] Using surface sensitive photoelectron spin-polarization measurement, strong evidence of the Fe surface live layer was observed in Fe/Co/Cu(100) system.[30] More interestingly, Dallmeyer *et al.* observed an oscillatory behavior of the Fe magnetization in Fe/Co/Cu(100), suggesting a complicated magnetic structure of the fcc Fe in the 4–11 ML thickness range.[31] Thus it is likely that the fcc Fe film in Fe/Co/Cu(100) is ferromagnetic live both at Fe/Co interface and at the Fe surface although the surface live layer may have a weaker magnetic signal at room temperature as compared with that at the Fe/Co interface. This may account for the controversial results reported from different groups. Nevertheless, it is shown that a fcc Fe film can mediate an oscillatory magnetic interlayer coupling between two ferromagnetic Co films.[27,31] Then if Cu and fcc Fe films are brought together to form a spacer layer, the Fe magnetic surface live layer will be sandwiched between the Cu and the antiferromagnetic fcc Fe films so that the role of the ferromagnetic live layer in the interlayer coupling can be investigated by varying the Cu and Fe film thicknesses. In this paper, we report the results of our study on the QW states and the interlayer coupling of Co/Cu/Fe/Co/Cu(100) where the Cu/Fe serves as the

spacer layer between the two ferromagnetic Co films. We found that the QW states of the spacer layer have little dependence on the Fe film thickness, no matter the Fe film is in fct ferromagnetic phase or fcc antiferromagnetic phase, but the magnetic interlayer coupling exhibits a checkerboard pattern in the Fe-Cu thickness plane. We explain the coupling result with the existence of the ferromagnetic live layer at Fe/Cu interface. To single out the importance of the ferromagnetic live layer in producing the checkerboard coupling pattern, we performed an experiment on Co/Cu/Co($\sim$1 ML)/Cu/Co/Cu(001) system, where the middle $\sim$1 ML Co in the spacer layer could be tuned by interlayer coupling and temperature to switch between paramagnetic and ferromagnetic states. We confirm that the checkerboard pattern of the interlayer coupling is associated with the ferromagnetic state of the middle Co film.

II. EXPERIMENT

The experiment was carried out at the Advanced Light Source (ALS) of the Lawrence Berkeley National Laboratory. The beamline 7.0.1.2 at the ALS can focus the photon beam down to $\sim$50 μm spot size with a high enough photon flux ($>10^{12}$ photons per second at resolving power of 10 000) to do photoemission measurement on wedged samples. For a wedge of $\sim$5 ML/mm slope, a scan of a 50 μm photon beam across the sample provides a systematic thickness-dependent measurement with $\sim$0.25 ML thickness resolution. A Cu(100) substrate of 1 cm diameter and 2 mm thickness was prepared by mechanical polishing down to 0.25 μm diamond paste, and followed by a chemical polishing.[32] The substrate was cleaned in an ultrahigh vacuum (UHV) system with cycles of 1–2 keV Ar ion sputtering and annealing at $\sim$600–700 °C. After cooling the substrate to room temperature, Co, Cu, and Fe films were epitaxially grown onto the Cu(100) substrate. The evaporation rate is calibrated by a quartz thickness monitor prior to the film growth. Typical growth rate of the film is $\sim$0.8 ML/min. A 10 ML Co film was grown first onto Cu(001) to serve as the ferromagnetic base layer. Double wedged spacer layers of Cu/Fe and Cu/Co/Cu were grown on top of the 10 ML Co by translating the substrate behind a knight-edge shutter in two orthogonal directions. Wedge slope is determined by the translating speed and the evaporation rate. After QW states were measured by ARPES, another 4 ML Co was grown on top of the spacer layer. After magnetizing the sample with a pulse magnetic field along the in-plane [011] direction to align the bottom 10 ML Co magnetization, the sample was measured by XMLD to study the oscillatory interlayer coupling.

For ARPES measurement, 83 eV photon energy was used to optimize the photoemission intensity at the Cu Fermi surface. The photoemission electrons were collected by a Scienta SES-100 analyzer with normal emission geometry. The total energy resolution is better than 60 meV at $\sim$1° angular acceptance. For XMLD measurement, 120 eV photon energy was used. The incident photon beam is *p* polarized with 60° incident angle (relative to the surface normal) and normal emission electrons are collected. Under this measurement geometry, the linear dichroism effect gives different Co 3*p* core-level spectra for the two opposite magnetization directions which are in the film plane but perpendicular to the photon incident plane[13]. Because of the surface sensitivity and that the bottom 10 ML Co was magnetized in one direction, the XMLD signal measures the magnetization direction of the top 4 ML Co, i.e., the sign of the interlayer coupling between the top 4 ML and the bottom 10 ML Co films across the spacer layer. The measurements were performed at room temperature, unless specifically mentioned.

III. RESULTS AND DISCUSSION

We first present the ARPES result of the Cu/Fe/Co/Cu(100) as a function of the Cu thickness at fixed Fe thickness. The Cu spectra for samples with 2 ML and 7 ML Fe thicknesses are shown in Figs. 1(a) and 1(b), and the spectra of Cu on Co layer is shown in Fig. 1(c) for comparison. The oscillations of the photoemission intensity with electron energy and the Cu film thickness show the presence of the QW states in the Cu film of Cu/Fe/Co/Cu(100). It was shown that the Cu QW states can be described very well with the quantization condition of $2(k_{BZ}-k)d_{Cu}-\Phi=2\pi\nu$, where Φ is the phase gain of the electron wave function upon reflections at the two Cu boundaries, d_{Cu} is the Cu thickness, ν is the quantum well index, k_{BZ} is the Brillouin vector, and k is the wave vector of the Cu *sp* band along the ΓX direction.[33] Thus the values of the wave vector k and the phase Φ at any given energy can be retrieved from the oscillations of the photoemission intensity versus the Cu film thickness. This essentially determines the energy dispersion $E-k$ (or energy band) and the phase Φ of the Cu film.[34] The results of $E-k$ and the phase Φ obtained from Figs. 1(a)–1(c). are shown in Figs. 1(d) and 1(e) We see that the $E-k$ are identical for Cu/Co/Cu(100), Cu/Fe(2 ML)/Co/Cu(100), and Cu/Fe(7 ML)/Co/Cu(100). This is expected because the $E-k$ represents the Cu *sp*-energy band and should be independent of the substrate materials. The phase Φ of the Cu QW state, however, is different for Cu/Fe/Co/Cu(100) and Cu/Co/Cu(100) [Fig. 1(e)]. This is because that the phase Φ depends on the electron reflection at the Cu/substrate interface so that the phase value should depend on substrate materials. It is interesting to note that the phase values of the QW states are identical for Cu/Fe(2 ML)/Co/Cu(100) and Cu/Fe(7 ML)/Co/Cu(100). It is well known that fcc Fe on Cu(100) has ferromagnetic phase below 4 ML and antiferromagnetic phase plus a ferromagnetic surface live layer between 4 and 11 ML. Thus it is somewhat "surprising" to see the same phase value in Cu/Fe(2 ML)/Co/Cu(100) and Cu/Fe(7 ML)/Co/Cu(100). To have a more accurate measurement, we performed experiment on Cu(wedge)/Fe(wedge)/Co/Cu(100) sample. Figure 2 shows the photoemission intensity at the Fermi level as a function of the Cu and Fe thicknesses. For Fe(wedge)/Co/Cu(100) ($d_{\mathrm{Cu}}=0$ ML), there is a clear change of the photoemission intensity at 4 ML Fe, indicating the ferromagnetic-to-antiferromagnetic transition. With Cu on top of the

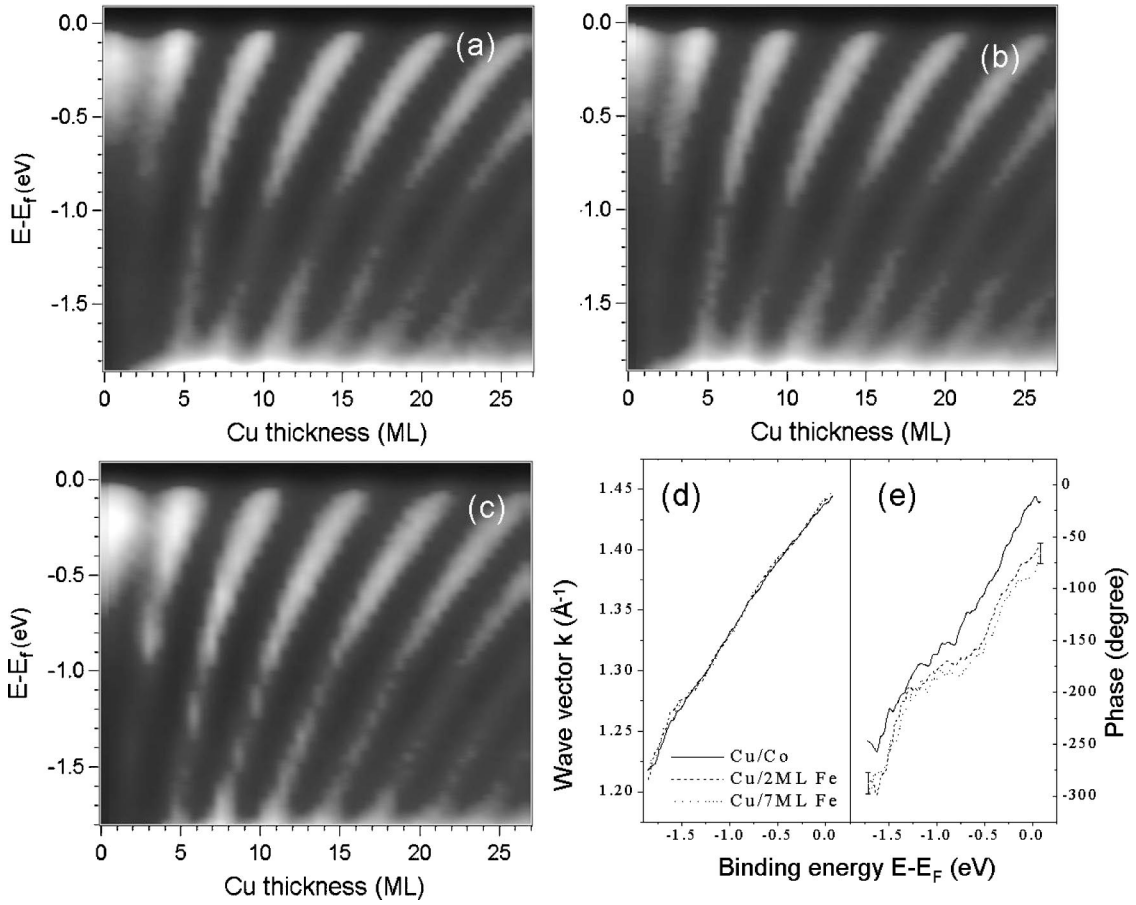

FIG. 1. Photoemission intensity normal to the film surface ($k_{//}=0$) vs the electron energy and the Cu film thickness for (a) Cu/Fe(2 ML)/Co(10 ML)/Cu(100), (b) Cu/Fe(7 ML)/Co(10 ML)/Cu(100), and (c) Cu/Co(10 ML)/Cu(100). (d) Dispersion of k vs E obtained from QW state fitting. (e) Quantization phase vs energy obtained from QW state fitting.

Fe/Co/Cu(100), the photoemission intensity of Cu/Fe/Co/Cu(100) oscillates as a function of the Cu thickness due to the QW states of Cu at E_F. The QW state positions shift slightly towards thinner Cu thickness as the Fe film thickness increases from 0 to ~1 ML. This is because the phase value of the QW states changes from that of Cu/Co interface to that of Cu/Fe interface. Thicker than 1 ML of Fe, the QW state positions remain fixed especially when crossing the ferromagnetic-to-antiferromagnetic phase transition at 4 ML of Fe. This result confirms that the quantum phase at the Cu/Fe interface is independent of the magnetic phase of the Fe film. Note that the fcc Fe film has a ferromagnetic surface live layer between 4 and 11 ML, the result of Fig. 2 indicates that the phase accumulation at the Cu/Fe interface is mainly determined by the electronic state of the Fe at the interface, i.e., the Cu electrons can not distinguish between the ferromagnetic fcc Fe below 4 ML and the ferromagnetic surface live layer of the fcc Fe between 4 and 11 ML.

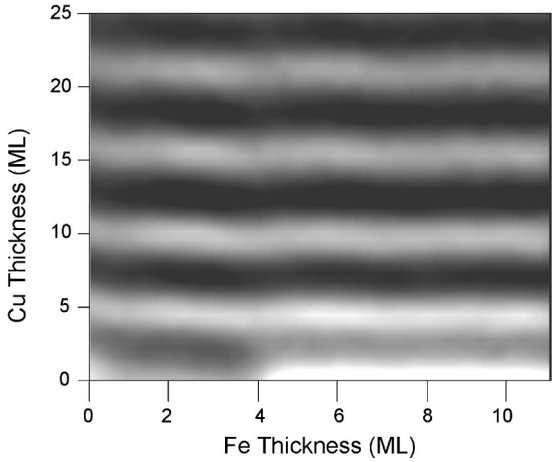

FIG. 2. Photoemission intensity at the Fermi level of Cu/Fe/Co(10 ML)/Cu(001) as a function of the Cu and Fe thicknesses.

We now discuss the result of interlayer coupling between two Co films across the Cu/Fe spacer layer. Figure 3 shows the XMLD measurement result on Co(4 ML)/Cu/Fe/Co(10 ML)/Cu(001) as a function of Cu and Fe thicknesses. The bright and dark regions correspond to the ferromagnetic coupling (FC) and antiferromagnetic coupling (AFC) between the 4 ML and 10 ML Co films, respectively. At $d_{Fe}=0$ ML, we observe the well-known oscillatory interlayer coupling of Co/Cu/Co/Cu(100) as a function of the Cu spacer layer thickness. For $0<d_{Fe}<4$ ML, the interlayer coupling pattern remains the same as in Co/Cu/Co sandwich

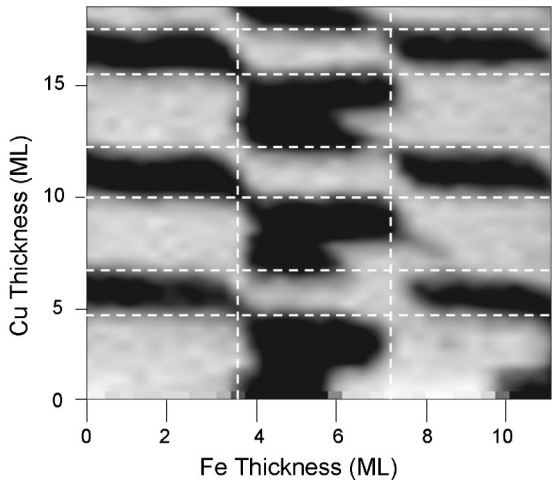

FIG. 3. Room temperature interlayer coupling, obtained from XMLD measurement, between the two Co films of Co(4 ML)/Cu/Fe/Co(10 ML)/Cu(100). The bright and dark regions correspond to the ferromagnetic- and antiferromagnetic-interlayer couplings. The interlayer coupling displays a checkerboard pattern. The white dashed lines are guide to eye to view the checkerboard pattern.

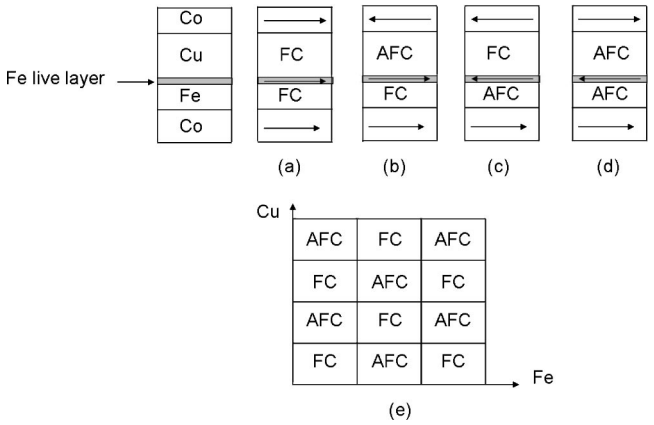

FIG. 4. (a)–(d) Four possible magnetization alignments of Co/Cu/Fe/Co/Cu(001). The arrows represent the magnetization directions of the Fe live layer and the Co films. (e) Checkerboard pattern of the interlayer coupling between the two Co films, resulting from the two-step couplings of Co-Fe(spacer)-Fe(live layer) and Fe(live layer)-Cu(spacer)-Co. "FC" and "AFC" denote for ferromagnetic coupling and antiferromagnetic coupling.

with the FC/AFC boundaries virtually unaffected by the Fe film. This is expected because the Fe film below 4 ML is in the ferromagnetic phase so that the interlayer coupling is sorely determined by the Cu film. For 4 ML $< d_{\mathrm{Fe}} <$ 11 ML, the antiferromagnetic Fe could serve as a spacer layer to generate oscillatory interlayer coupling. This can be clearly seen in Fig. 3 at $d_{\mathrm{Cu}}=0$ ML where the interlayer coupling oscillates as a function of Fe film thickness in Co/Fe/Co/Cu(100). For antiferromagnetic Fe, the interlayer coupling across Cu/Fe spacer layer exhibits interesting pattern. At any fixed Fe thickness, the interlayer coupling oscillates with the Cu thickness with the same periodicity as in Co/Cu/Co/Cu(100). However, the sign of the coupling across the Cu/Fe spacer is reversed if the corresponding Fe thickness produces an AFC in Co/Fe/Co/Cu(100). This coupling character produces a checkerboard coupling pattern (Fig. 3) in the Fe-Cu thickness plane (except a small distortion in the range of 6 ML $< d_{\mathrm{Fe}} <$ 7 ML). For nonmagnetic spacer, the interlayer coupling is usually explained with the spin polarized QW states of the spacer layer.[11] This scenario of interlayer coupling leads to a continuous evolution of the AFC position in concise with the QW sates at the Fermi level. Experiment on interlayer coupling across $Cu/Ni_{30}Cu_{70}$ spacer layer confirms this kind of evolution that the AFC position shifts linearly in the $Cu\text{-}Ni_{30}Cu_{70}$ thickness plane according to the QW states at the Fermi level.[21] This coupling picture cannot explain the checkerboard pattern of Fig. 3, which is very different from the diagonal pattern as observed in the $Cu/Ni_{30}Cu_{70}$ spacer layer case. Noticing the difference of *nonmagnetic* $Ni_{30}Cu_{70}$ and the *magnetic* fcc Fe, the checkboard pattern of Fig. 3 must be related to the magnetic nature of the fcc Fe.

As discussed earlier, room temperature grown fcc Fe film on Co(001) is ferromagnetic below 4 ML and antiferromagnetic plus a ferromagnetic live layer between 4 and 11 ML, but the Curie temperature depends on the growth condition sensitively. For Fe/Cu(001) system, it is shown that after capping the film with a Cu layer the Fe live layer survives but with a lowered Curie temperature.[35] It is reasonable to assume that the live surface layer in fcc Fe/Co(001) system also survives after capping the film with a Cu layer although its magnetic moment may be much weaker than that at the Fe/Co interface at room temperature.[36] On the other hand, it has been shown recently that the ferromagnetic order of one film in a magnetically coupled sandwich could enhance the Curie temperature of the other film.[37,38] Therefore the top Co film in the Co/Cu/Fe/Co/Cu(100) is expected to enhance the magnetic order of the Fe live layer at the Cu/Fe interface by interlayer coupling. Assuming that there indeed exists such Fe ferromagnetic live layer at the Cu/Fe interface at room temperature, the checkerboard pattern shown in Fig. 3 can be explained with a simple physical picture. The sample structure can be considered as sketched in Fig. 4 where there is a Fe ferromagnetic live layer at the Cu/Fe interface. The thick bottom Co layer serves as a magnetic base layer whose magnetization direction is fixed. The direction of the Fe ferromagnetic live layer at the Cu/Fe interface is determined by the interlayer coupling between the fcc Fe live layer and the bottom Co layer across the fcc Fe spacer. The magnetization direction of the top Co layer is subsequently determined by the interlayer coupling between the top Co layer and the fcc Fe ferromagnetic live layer across the Cu spacer. Then the final coupling between the top and bottom Co films are determined by two steps of Co-Cu-Fe(live layer) coupling and Fe(live layer)-Fe(spacer)-Co coupling. As a result, there are four magnetic configurations as shown in Figs. 4(a)–4(d). For $d_{\mathrm{Fe}} <$ 4 ML, the Fe layer is ferromagnetic so that the coupling in Co/Cu/Fe/Co has the same sign as that in Co/Cu/Co. For 4 ML $< d_{\mathrm{Fe}} <$ 6 ML, the Fe live layer is antiferromagnetically coupled to the bottom Co layer so that the final coupling between the top and the bottom Co layers across the Fe/Cu spacer has an opposite sign to that of

Co/Cu/Co. Based on this model, the coupling between the two Co films across the Cu/Fe spacer can be easily constructed as shown in Fig. 4(e) which agrees reasonably well with the checkerboard pattern of Fig. 3.

The above simple coupling model requires the ferromagnetic order of the Fe at the Cu/Fe interface even though the magnetic moment could be weak. In other words, the two steps of Co-Cu-Fe(live layer) and Fe(live layer)-Fe(spacer)-Co couplings should switch to a direct single step coupling of Co-Cu/Fe-Co if the magnetic order of the Cu/Fe interfacial live layer disappears. To confirm this assertion, we designed an experiment to study the interlayer coupling of Co(4 ML)/Cu(top)/Co(1.3 ML)/Cu(bottom)/Co(10 ML)/Cu(001) in which the Cu(top)/Co(1.3 ML)/Cu(bottom) serves as the spacer layer. Compared with the Co/Cu/Fe/Co/Cu(100), the middle 1.3 ML Co can be regarded as an artificial ferromagnetic live layer. Thus if the 1.3 ML Co is in the ferromagnetic state (though it could be weak), the coupling between the 4 ML and 10 ML Co films should go through two steps of Co(4 ML)/Cu(top)/Co(1.3 ML) coupling and Co(1.3 ML)/Cu(bottom)/Co(10 ML) coupling, and the final coupling between the 4 ML and 10 ML Co films should display a checkerboard pattern in the Cu(top)-Cu(bottom) thickness plane. If the 1.3 ML Co is in the paramagnetic state, the 1.3 ML Co would serve as a spin-independent spacer so that the coupling between the 4 ML and 10 ML Co films should go through a single step coupling across the Cu(top)/Co(1.3 ML)/Cu(bottom) spacer to result in a continuous diagonal evolution of the interlayer coupling in a similar way as in the $Co/Cu/Ni_{30}Cu_{70}/Cu/Co/Cu(100)$ case. We chose 1.3 ML Co in the middle because its magnetic state at room temperature can be tuned by the interlayer coupling. For Co film grown on Cu(001), the Co film is ferromagnetic above 1.5 ML and paramagnetic below 1.5 ML at room temperature.[39] The critical thickness value of 1.5 ML shifts to ~2 ML for Cu/Co/Cu(100).[38] However, it is shown that interlayer coupling in a magnetically coupled sandwich decreases the critical thickness of the paramagnetic-to-ferromagnetic phase transition.[36,38] For example, the coupling across a 2 ML Cu spacer in Cu/Co/Cu/Ni/Cu(100) sandwich decreases the Co critical thickness from 2 ML to 0.9 ML. Since the coupling strength depends on the spacer layer thickness, the middle 1.3 ML Co will be in the ferromagnetic state for thinner Cu spacer and in the paramagnetic state for thicker Cu spacer. Figure 5 shows the interlayer coupling result of Co(4 ML)/Cu(top)/Co(1.3 ML)/Cu(bottom)/Co(10 ML)/Cu(001) in the Cu(top)-Cu(bottom) thickness plane. For Cu thickness thinner than ~15 ML, the coupling forms a checkerboard pattern. This is because the 1.3 ML Co carries certain degree of ferromagnetic order so that the coupling between the 4 ML and 10 ML Co films is by two steps of (4 ML)/Cu(top)/Co(1.3 ML) coupling and Co(1.3 ML)/Cu(bottom)/Co(10 ML) coupling. For Cu thickness thicker than ~15 ML, the coupling forms a diagonal pattern in the Cu(top)-Cu(bottom) thickness plane. This is because the 1.3 ML Co is in the paramagnetic state

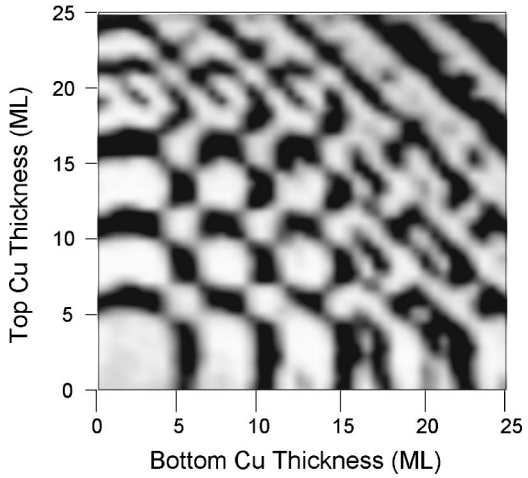

FIG. 5. Room temperature interlayer coupling, obtained from XMLD measurement, between the 4 ML and 10 ML Co films of Co(4 ML)/Cu/Co(1.3 ML)/Cu/Co(10 ML)/Cu(100). The bright and dark regions correspond to the ferromagnetic- and antiferromagnetic interlayer couplings. The interlayer coupling displays a checkerboard pattern below ~15 ML Cu thickness, and a diagonal pattern above ~15 ML Cu.

so that the coupling between the 4 ML and 10 ML Co films is through a single step coupling across the Cu(top)/Co(1.3 ML)/Cu(bottom) spacer (thus depends on the total Cu thickness only).

Temperature-dependence measurement was also carried out on Co(4 ML)/Cu(top)/Co(1.1 ML)/Cu(bottom)/Co(10 ML)/Cu(001). The XMLD measurement was first performed on Co(1.1 ML)/Cu/Co(10 ML)/Cu(001) at room temperature and low temperature (T=82 K). Figure 6(a) shows XMLD signal from the 3p level of the 1.1 ML Co as a function of the Cu thickness. At low temperature, the oscillation of the XMLD signal versus the Cu thickness shows that the 1.1 ML Co is in ferromagnetic state and its magnetic direction alternates as a function of the Cu thickness due to the interlayer coupling between the 1.1 ML Co and the 10 ML Co. At room temperature, the XMLD signal of the 1.1 ML Co disappears above 5 ML Cu, showing that the 1.1 ML Co is in paramagnetic state. Although we cannot determine the magnetic order of the 1.1 ML Co layer after growing the Co(4 ML)/Cu(top wedge) because of the surface sensitivity of the XMLD measurement, we believe that the middle 1.1 ML Co remains its ferromagnetic phase at low temperature and paramagnetic phase at room temperature. Thus the interlayer coupling between the 4 ML and 10 ML Co films across the Cu/(top)/Co(1.1 ML)/Cu(bottom) spacer layer should change from diagonal pattern at room temperature to checkerboard pattern at low temperature in the Cu(top)-Cu(bottom) thickness plane. This prediction was proved by our experimental results, as shown in Figs. 6(b) and 6(c). As expected, the coupling between the 4 ML and 10 ML Co films displays a diagonal pattern in the Cu(top)-Cu(bottom) thickness plane above 5 ML Cu at room temperature [Fig. 6(b)], and evolves into the checkerboard pattern [Fig. 6(c)] at low temperature (especially in the 7–12 ML Cu thickness range). It should be

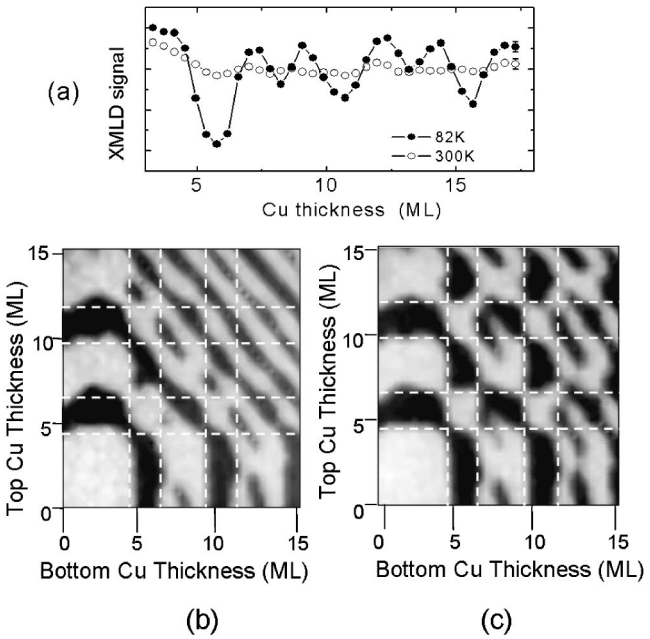

FIG. 6. (a) Co XMLD signal of Co(1.1 ML)/Cu/Co(10 ML)/Cu(100) vs the Cu thickness at room temperature (open dots) and 82 K (solid dots). (b) and (c) XMLD measurement of the interlayer coupling between the 4 ML and 10 ML Co films of Co(4 ML)/Cu/Co(1.1 ML)/Cu/Co(10 ML)/Cu(100) at (b) room temperature and (c) $T=82$ K. The bright and dark regions correspond to the ferromagnetic- and antiferromagnetic-interlayer couplings. The diagonal pattern at room temperature evolves into checkerboardlike pattern at low temperature. The white dashed lines are guide to eye to see the evolution.

mentioned that the results shown in Figs. 6(b) and 6(c) are reversible, i.e., the coupling recovers to the diagonal pattern of Fig. 6(b) after warming up the sample back to room temperature. It is also worthy to mention the presence of the short-period oscillations of the interlayer coupling,[13] which indicates a high quality of our samples.

The results of Figs. 5 and 6 confirm that the ferromagnetic order of the middle Co layer plays a key role in establishing the checkerboard pattern of the interlayer coupling. However, it is still an open question on the required magnitude of the middle layer magnetic moment to cross from the diagonal coupling pattern to the checkerboard coupling pattern. Nevertheless, the experiment on Co/Cu/Co/Cu/Co/Cu(100) system explains that the checkerboard pattern of Fig. 3 is related to the ferromagnetic live layer of the fcc Fe film at the Cu/Fe interface. Since the XMLD measures only the sign of the interlayer coupling, it remains unexplored on the relationship between the checkerboard pattern and the interlayer coupling strength. It is reported that the QW states at the Fermi level is modulated by the position of a middle Ni layer in Cu/Ni(1 ML)/Cu/Co/Cu(001) system.[41] The same effect was also observed in Cu/Co(1 ML)/Cu/Co/Cu(001) system.[41] Then it would be very interesting to study systematically how the interlayer coupling, both the sign and the strength, depends on the middle Co layer thickness in Co/Cu/Co/Cu/Co/Cu(001). This could be a future project.

IV. SUMMARY

We investigated the Cu QW states and the interlayer coupling in Co(4 ML)/Cu/Fe/Co(10 ML)/Cu(100) by APRES and XMLD. The Cu QW states are independent of the magnetic states of the fcc Fe film. The interlayer coupling between the 4 ML and 10 ML Co films displays a checkerboard pattern in the Cu-Fe thickness plane. The presence of ferromagnetic live layer of the fcc Fe film at the Cu/Fe interface explains the checkerboard pattern by a two-step coupling mechanism. Experiments on Co(4 ML)/Cu/Co/Cu/Co(10 ML)/Cu(001) system confirm that the ferromagnetic state of the middle Co layer is needed to establish the checkerboard pattern of the interlayer coupling.

ACKNOWLEDGMENTS

This work was supported by National Science Foundation under Contract No. DMR-0110034, the U.S. Department of Energy under Contract No. DE-AC03-76SF00098, and the ICQS of Chinese Academy of Sciences.

[1] P. Grünberg, R. Schreiber, Y. Pang, M. B. Brodsky, and H. Sowers, Phys. Rev. Lett. **57**, 2442 (1986).
[2] S. S. P. Parkin, N. More, and K. P. Roche, Phys. Rev. Lett. **64**, 2304 (1990).
[3] P. J. H. Bloemen, M. T. Johnson, M. T. H. van de Vorst, R. Coehoorn, J. J. de Vries, R. Jungblut, J. aan de Stegge, A. Reinders, and W. J. M. de Jonge, Phys. Rev. Lett. **72**, 764 (1994).
[4] S. N. Okuno and K. Inomata, Phys. Rev. Lett. **72**, 1553 (1994).
[5] S. N. Okuno and K. Inomata, Phys. Rev. B **51**, 6139 (1995).
[6] J. E. Ortega and F. J. Himpsel, Phys. Rev. Lett. **69**, 844 (1992).
[7] P. Segovia, E. G. Michel, and J. E. Ortega, Phys. Rev. Lett. **77**, 3455 (1996).
[8] R. Klasges, D. Schmitz, C. Carbone, W. Eberhardt, P. Lang, R. Zeller, and P. H. Dederichs, Phys. Rev. B **57**, R696 (1998).
[9] M. Schifgarrde and W. Harrison, Phys. Rev. Lett. **71**, 3870 (1993).
[10] B. A. Jones and C. B. Hanna, Phys. Rev. Lett. **71**, 4253 (1993).
[11] P. Bruno, Europhys. Lett. **23**, 615 (1993).
[12] R. K. Kawakami, E. Rotenberg, Ernesto J. Escorcia-Aparicio, Hyuk J. Choi, T. R. Cummins, J. G. Tobin, N. V. Smith, and Z. Q. Qiu, Phys. Rev. Lett. **80**, 1754 (1998).
[13] R. K. Kawakami, E. Rotenberg, Ernesto J. Escorcia-Aparicio, Hyuk J. Choi, J. H. Wolfe, N. V. Smith, and Z. Q. Qiu, Phys. Rev. Lett. **82**, 4098 (1999).
[14] J. G. J. Strijkers, J. T. Kohlhepp, H. J. M. Swagten, and W. J. M. de Jonge, Phys. Rev. Lett. **84**, 1812 (2000).
[15] R. W. E. van de Kruijs, M. Th. Rekveldt, H. Fredrikze, J. T. Kohlhepp, J. K. Ha, and W. J. M. de Jonge, Phys. Rev. B **65**, 064440 (2002).

[16] C. L. Platt, M. R. McCartney, F. T. Parker, and A. E. Berkowitz, Phys. Rev. B **61**, 9633 (2000)
[17] J. Faure-Vincent, C. Tiusan, C. Bellouard, E. Popova, M. Hehn, F. Montaigne, and A. Schuhl, Phys. Rev. Lett. **89**, 107206 (2002).
[18] M. Kowalewski, B. Heinrich, J. F. Cochran, and P. Schurer, J. Appl. Phys. **81**, 3904 (1997).
[19] D. E. Bürgler, F. Meisinger, C. M. Schmidt, D. M. Schaller, H.-J. Güntherodt, and P. Grünberg, Phys. Rev. B **60**, R3732 (1999).
[20] C. L. Platt, M. R. McCartney, F. T. Parker, and A. E. Berkowitz, Phys. Rev. B **61**, 9633 (2000).
[21] Z. D. Zhang, Hyuk J. Choi, R. K. Kawakami, Ernesto J. Escorcia-Aparicio, M. O. Bowen, J. H. Wolfe, E. Rotenberg, N. V. Smith, and Z. Q. Qiu, Phys. Rev. B **61**, 76 (2000).
[22] D. Pescia, M. Stampanoni, G. L. Bona, A. Vaterlaus, R. F. Willis, and F. Meier, Phys. Rev. Lett. **58**, 2126 (1987).
[23] P. A. Montano, G. W. Fernando, B. R. Cooper, E. R. Moog, H. M. Naik, S. D. Bader, Y. C. Lee, Y. N. Darici, H. Min, and J. Marcano, Phys. Rev. Lett. **59**, 1041 (1987).
[24] J. Thomassen, F. May, B. Feldmann, M. Wuttig, and H. Ibach, Phys. Rev. Lett. **69**, 3831 (1992).
[25] D. Li, M. Freitag, J. Pearson, Z. Q. Qiu, and S. D. Bader, Phys. Rev. Lett. **72**, 3112 (1994).
[26] W. L. O'brien and B. Tonner, Phys. Rev. B **52**, 15 332 (1996); W. L. O'Brien and B. P. Tonner, Surf. Sci. **334**, 10 (1995).
[27] E. J. Escorcia-Aparicio, R. K. Kawakami, and Z. Q. Qiu, Phys. Rev. B **54**, 4155 (1996).
[28] X. Y. Gao, M. Salvietti, W. Kuch, C. M. Schneider, and J. Kirschner, Phys. Rev. B **58**, 15 426 (1998)
[29] D. Schmitz, C. Charton, A. Scholl, C. Carbone, and W. Eberhardt, Phys. Rev. B **59**, 4327 (1999)
[30] R. Kläsges, D. Schmitz, C. Carbone, W. Eberhardt, and T. Kachel, Solid State Commun. **107**, 13 (1998); A. Kakizaki, N. Kamakurra, M. Sawada, K. Hayashi, and T. Saitoh, Surf. Rev. Lett. **7**, 667 (2000).
[31] A. Dallmeyer, K. Maiti, O. Rader, L. Pasquali, C. Carbone, and W. Eberhardt, Phys. Rev. B **63**, 104413 (2001).
[32] W. J. McG.Tegart, *The Electrolytic and Chemical Polishing of Metals in Research and Industry* (Pergamon Press, New York, 1959); W. Heppler, LBNL Report No. 3078 1989 (unpublished).
[33] N. V. Smith, N. B. Brookes, Y. Chang, and P. D. Johnson, Phys. Rev. B **49**, 332 (1994).
[34] J. M. An, D. Raczkowski, Y. Z. Wu, C. Y. Won, L. W. Wang, A. Canning, M. A. Van Hove, E. Rotenberg, and Z. Q. Qiu, Phys. Rev. B **68**, 045419 (2003).
[35] R. Vollmer, S. van Dijken, M. Schleberger, J. Kirschner, Phys. Rev. B **61**, 1303 (2000).
[36] Y. Z. Wu, C. Won, A. Scholl, A. Doran, F. Toyoma, X. F. Jin, N. V. Smith, and Z. Q. Qiu, Phys. Rev. B **65**, 214417 (2002).
[37] U. Bovensiepen, F. Wilhelm, P. Srivastava, P. Poulopoulos, M. Farle, A. Ney, and K. Baberschke, Phys. Rev. Lett. **81**, 2368 (1998).
[38] C. Won, Y. Z. Wu, A. Scholl, A. Doran, N. Kurahashi, H. W. Zhao, and Z. Q. Qiu, Phys. Rev. Lett. **91**, 147202 (2003).
[39] Q. Y. Jin, H. Regensburger, R. Vollmer, and J. Kirschner, Phys. Rev. Lett. **80**, 4056 (1998).
[40] R. K. Kawakami, E. Rotenberg, Hyuk J. Choi, Ernesto J. Escorcia-Aparicio, M. O. Bowen, J. H. Wolfe, E. Aronholtz, Z. Zhang, N. V. Smith, and Z. Q. Qiu, Nature (London) **398**, 132 (1999).
[41] W. L. Ling, E. Rotenberg, H. J. Choi, J. H. Wolfe, F. Toyama, S. Paik, N. V. Smith, and Z. Q. Qiu, Phys. Rev. B **65**, 113406 (2002).